

## Origin and development of the zebrafish endoderm

Rachel M. Warga\*<sup>‡</sup> and Christiane Nüsslein-Volhard

Max-Planck-Institut für Entwicklungsbiologie, Abteilung Genetik, Spemannstrasse 35, 72076 Tübingen, Germany

\*Present address: University of Rochester, Department of Biology, Rochester NY 14627-0211, USA

<sup>‡</sup>Author for correspondence (e-mail: rachel\_warga@urmc.rochester.edu)

Accepted 8 December 1998; published on WWW 20 January 1999

### SUMMARY

The segregation of cells into germ layers is one of the earliest events in the establishment of cell fate in the embryo. In the zebrafish, endoderm and mesoderm are derived from cells that involute into an internal layer, the hypoblast, whereas ectoderm is derived from cells that remain in the outer layer, the epiblast. In this study, we examine the origin of the zebrafish endoderm and its separation from the mesoderm. By labeling individual cells located at the margin of the blastula, we demonstrate that all structures that are endodermal in origin are derived predominantly from the more dorsal and lateral cells of the blastoderm margin. Frequently marginal cells give rise to both endodermal and mesodermal derivatives, demonstrating that these two lineages have not yet separated. Cells located farther than 4 cell diameters from the margin give rise exclusively to mesoderm, and not to endoderm.

Following involution, we see a variety of cellular changes

indicating the differentiation of the two germ layers. Endodermal cells gradually flatten and extend filopodial processes forming a noncontiguous inner layer of cells against the yolk. At this time, they also begin to express Forkhead-domain 2 protein. Mesodermal cells form a coherent layer of round cells separating the endoderm and ectoderm.

In *cyclops*-mutant embryos that have reduced mesodermal anlage, we demonstrate that by late gastrulation not only mesodermal but also endodermal cells are fewer in number. This suggests that a common pathway initially specifies germ layers together before a progressive sequence of determinative events segregate endoderm and mesoderm into morphologically distinct germ layers.

Key words: Endoderm, Mesoderm, Fate map, Single cell labeling, Morphogenesis, Germ layer, *cyclops*.

### INTRODUCTION

Formation of the vertebrate body plan begins with the segregation of cells into germ layers. An important question in developmental biology is how these germ layers arise from an initially homogeneous population of cells. While considerable work has focused on the cellular and molecular mechanisms by which the ectoderm and mesoderm become different, we know very little about formation of the endoderm. Increasingly it is becoming clear that endoderm has an important role during early patterning. In frogs, cells of the endoderm are derived from a region that acts as a signalling center to induce the Spemann organizer (Nieuwkoop, 1969). Moreover, dorsal endoderm, as part of the organizer in mouse, chick and frog, participates in patterning heart mesoderm and anterior neural ectoderm (Nascone and Marcola, 1995; Story et al., 1995; Shimamura and Rubenstein, 1997). By understanding the timing and factors that lead to emergence of the endodermal layer, we can better understand the interactions that occur between different cell populations during vertebrate morphogenesis.

In all vertebrates studied, the endoderm and mesoderm seem to have many similarities in their early development. Both germ layers derive from cells that express the same regulatory

genes (Papaioannou and Silver, 1998; Hammerschmidt and Nüsslein-Volhard, 1993) before undergoing internalization during early gastrulation. Additionally, during their initial patterning, precursors to both germ layers respond to some of the same signalling molecules (Henry et al., 1996; Sasai et al., 1996; Hudson et al., 1998). In *Xenopus*, where endoderm development has been best characterized, clonal analysis shows that endoderm originates from superficial cells around the equator of the blastula before gastrulation. While a minority of these cells also contribute to mesoderm indicating that some endoderm and mesoderm co-localize, the great majority of mesoderm derives from closely opposed deeper cells at the same latitude (Keller, 1975, 1976; Minsuk and Keller, 1997). By mid-gastrulation, after equatorial cells have involuted, the germ layers become morphologically distinct. At about the same time, endoderm cells become irreversibly committed (Wylie et al., 1987) and molecular characterization suggests that each germ layer is expressing a specific set of mutually exclusive genes (Henry and Melton, 1998; Lemaire et al., 1998). Fate maps in urodeles and other anurans, as well as higher vertebrates, likewise show that endoderm and mesoderm both originate, albeit more extensively than *Xenopus*, from overlapping regions of the blastula (Delarue et al., 1992; Hatada and Stern, 1994; Lawson et al., 1991; Minsuk

and Keller, 1997). Moreover, until after cells ingress, the germ layers are not apparent.

In the zebrafish embryo, endoderm and mesoderm also appear to originate from a shared location. Both germ layers derive from cells near the blastoderm margin (Kimmel et al., 1990), and both involute into the forming hypoblast (Warga and Kimmel, 1990) where, at least initially, they are indistinguishable by either molecular or morphological criteria. However, there is some bias in the distribution of precursors: earlier involuting cells predominantly form endoderm and later involuting cells form mesoderm (Warga and Kimmel, 1990). While detailed fate maps exist for the mesoderm and neural ectoderm (Kimmel et al., 1990; Stainier et al., 1993; Lee et al., 1994; Woo and Fraser, 1995; Shih and Fraser, 1995; Melby et al., 1996), no similar map exists for the endoderm.

This report describes the origin of the endoderm in the zebrafish and its cellular differentiation from mesoderm. By labeling single cells at the margin of the early blastula, we show that endodermal and mesodermal precursors are distributed throughout the margin of the blastoderm and often share a common precursor. Endodermal structures derive chiefly from the dorsal and lateral margin. By mid-gastrulation, cells becoming endoderm begin to acquire a unique morphology, and occupy the deepest hypoblast location, consistent with cellular differentiation into a definitive germ layer.

We have also examined some of the molecular changes that precede or accompany segregation into the endodermal germ layer. In mouse, the genes *HNF3 $\alpha$*  and *HNF3 $\beta$*  are expressed in definitive endoderm, as well as notochord (Ang et al., 1993; Monaghan et al., 1993; Sasaki and Hogan, 1993), and chimeric studies in mice with a targeted deletion of the *HNF3 $\beta$*  gene demonstrate that *HNF3 $\beta$*  is required for specification of foregut and midgut endoderm (Dufort et al., 1998). HNF3-proteins belong to a family of transcription factors with a winged helix DNA-binding domain, related to the *Drosophila* gene *fork head*. In zebrafish, a family of nine *fork head* genes has been described (Strähle et al., 1993; Dirksen and Jamrich, 1995; Odenthal and Nüsslein-Volhard, 1998), however, *forkhead-domain 2* (*fkd2*), the homologue of mouse *HNF3 $\gamma$* , appears to be the only member of this family that becomes developmentally restricted to cells of the differentiating gut (Odenthal and Nüsslein-Volhard, 1998). Here, we use a Fkd2 antibody to describe the establishment of the endodermal germ layer showing that Fkd2 protein is already expressed before endodermal precursors become morphologically distinct.

Lastly, to further understand the steps involved in endoderm specification, we have analyzed endoderm development in embryos mutant for the gene *cyclops*, encoding a *nodal*-related signalling molecule expressed in presumptive endoderm and mesoderm (Rebagliati et al., 1998; Sampath et al., 1998). Previous studies have indicated that *cyclops*-mutant embryos are missing dorsally derived neuroectoderm (Hatta et al., 1991, 1994; Strähle et al., 1993). Less severe reductions are found in some dorsal mesodermal precursors (Thisse et al., 1994). Consistent with the idea that endoderm and mesoderm share many similarities during early gastrulation, we find that, in embryos mutant for *cyclops*, the endodermal precursors are reduced. Our results indicate that before morphological events segregate endoderm into a germ layer, a common pathway specifies both the endoderm and mesoderm.

## MATERIALS AND METHODS

### Embryos

Normal cell fates were traced either in wild-type embryos, or homozygous *golden<sup>bl</sup>* embryos, a mutation that reduces melanin and, thus, provides greater optical clarity in older embryos, but otherwise develops normally (Warga and Kimmel, 1990; Kimmel et al., 1990). In addition, some of the parents were heterozygous for *spadetail*; data for homozygous mutant progeny is presented elsewhere (Warga and Nüsslein-Volhard, 1998). To trace cell fates in *cyclops* mutants, embryos were derived from crosses of identified *cyclops<sup>b16</sup>* heterozygotes. Embryos were staged by morphology during the first 24 hours (Kimmel et al., 1995) and, after that, by time postfertilization at 28°C.

### Making the fate map

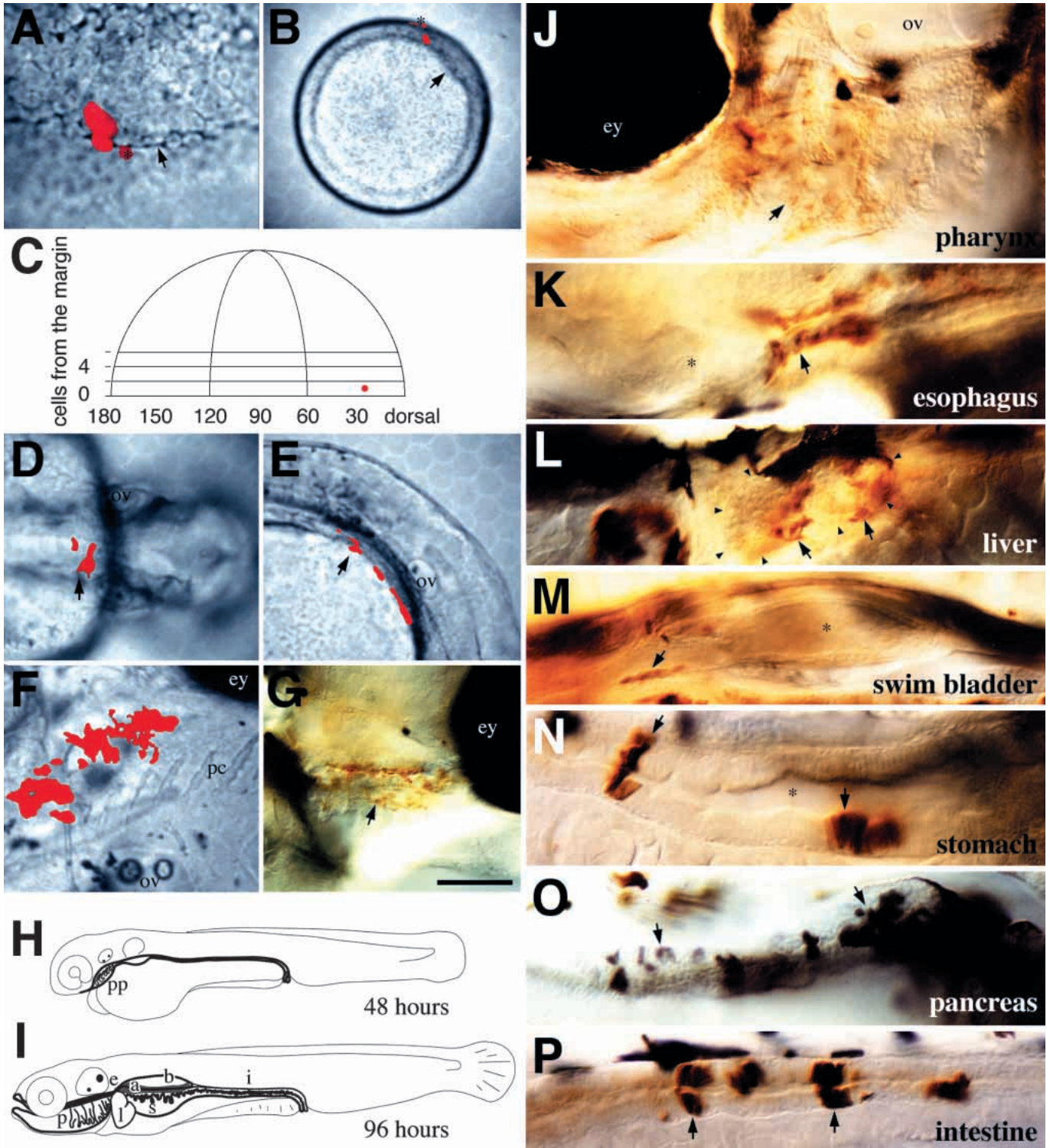
Between the 1000- to 4000-cell stage, single marginal cells (between 1 and 3 cell diameters from the blastoderm margin) were co-injected with a mixture of 5% rhodamine-dextran (Warga and Kimmel, 1990) and 2% biotinylated-dextran (Molecular Probes), a fixable tracer.

For this study, a total of 289 embryos were injected, 71 of which were used in creating the fate map. On average, 12 embryos were injected per experiment-day, and typically only 5±3 embryos used for

**Fig. 1.** The method used for making the fate map for endoderm. A single cell on the blastoderm margin was co-injected with rhodamine- and biotin-dextran at mid-blastula (1000-cell stage, 3 hours). (A) At 40% epiboly, the clone (now 4 deep cells and 1 enveloping layer cell; asterisk) was examined in face view. The distance of each cell from the blastoderm margin (arrow) was measured in terms of cell diameters. In this clone, one cell lies just below the margin and was designated in tier 0, the other cells were in tiers 1 and 2. (B) At shield stage, the clone was re-examined from an animal pole view. Frequently, the number of deep cells was the same. The distance between the dorsal midline (arrow) and the center of the clone was measured in degrees of arc. By now, all labeled deep cells had involuted; asterisk, enveloping layer cells. (C) Depiction of the blastoderm at 40% epiboly and the position of the mapped clone. Although the clone was on the right, it is projected to the left side of the blastoderm for conventional presentation (Kimmel et al., 1990). (D,E) At 30 hours, the deep cell clone formed part of an epithelial layer overlying the yolk sac. (D) Dorsal view. (E) Lateral view. The arrow indicates the same group of cells. (F,G) By 96 hours, the deep cell clone had become pharyngeal endoderm within the gills. (F) Ventral oblique view of the live embryo, anterior to the right. The clone, between the right eye and left ear, was near pharyngeal cartilage. (G) Lateral view, after whole-mount staining for the fixable tracer. The cells of the endodermal clone, now stained brown (arrow), formed a simple squamous epithelium covering the gills. (H,I) Depiction of the developing digestive tract (bold outline). (H) At 48 hours, the gut tube. Only the pharyngeal pouches, early pharynx, have noticeably differentiated. (I) At 96 hours, the gut is fully differentiated. The subdivisions include (progressing rostro-caudally): the pharynx (including gills), the esophagus, the stomach and the intestine. The liver (left), swimbladder (medial), and pancreas (right; shaded) are diverticula of the gut. (J-P) Whole-mount-stained clones between 96 and 120 hours of development illustrating differentiated endodermal tissues. (J-M,P) are left side presentations, (N,O) are right side; arrows indicate labeled cells within each structure; asterisks indicate lumens. (J) Pharynx: simple squamous epithelium. (K) Esophagus: stratified squamous epithelium. (L) Liver (outlined in arrowheads): parenchymal cells. (M) Swimbladder: pseudostratified squamous epithelium. (N) Stomach: simple columnar epithelium. (O) Pancreas: parenchymal cells containing prominent vesicles (putative zymogen granules). (P) Intestine: simple columnar epithelium. Scale bar: 50  $\mu$ m (A,F,G), 200  $\mu$ m (B), 100  $\mu$ m (D,E), 25  $\mu$ m (J-P). Abbreviations: a, pancreas; b, swimbladder; e, esophagus; i, intestine; l, liver; p, pharynx; s, stomach; ey, eye; ov, ear; pc, pharyngeal cartilage; pp, pharyngeal pouches.

the fate map data set. Embryos were excluded from this study due to (1) early lethality (29%), (2) labeling a clone of enveloping layer cells (12%), (3) dye coupling to the yolk cell, damage to the clone, dimness of the clone or embryonic abnormalities (11%), or (4) labeling a clone in an embryo homozygous mutant for *spadetail* (23%; Warga and Nüsslein-Volhard, 1998). Labeled clones are designated by our laboratory book number. In some cases, an injected cell was dye-coupled to a sister cell, producing a brightly labeled clone and a dimly labeled clone, these are designated as clone (a) and (b).

The distance between the clone and the margin was mapped about 1 hour after labeling, when embryos were at 40% epiboly, before the dorsal side is apparent. At this time, the blastoderm is composed of two cell populations: flattened enveloping layer cells, in a surface monolayer, and loosely associated deep cells, forming a 4- to 6-cell-thick layer, which gives rise to the embryo proper. Enveloping layer cells give rise to periderm (Kimmel et al., 1990) and were not followed in these studies. We mounted embryos in 3% methyl cellulose, recording the position of all labeled deep cells (Fig. 1A). By this time,



there were usually 4 cells ( $3.7 \pm 0.22$  cells) per clone and the longest dimension of the clone was normally 2 to 4 cells. We took the average position of all the deep cells within the clone to give us the geometric distance of the center of the clone from the margin (Fig. 1C).

To measure the distance from the clone to the dorsal midline, we examined each clone again at shield stage when the dorsal side of the embryo becomes visible (Fig. 1B). This gave us the angular distance between the clone and the dorsal midline (Fig. 1C). In a subset of these embryos, we additionally reexamined the location of labeled cells with respect to the margin.

All progeny of these labeled cells were again examined at 24 hours (Fig. 1D,E). Labeled cells were followed for up to 5 days of development to determine which differentiated structures they populated (Fig. 1F). Embryos were fixed and stained, allowing for further analysis of cell morphology and location of the clonally derived cells (Fig. 1G).

### Identification of endodermal and mesodermal precursors

A subset of the labeled embryos was also carefully examined throughout gastrulation. Beginning at 70% epiboly, embryos were mounted as described above and clonally related cells were analyzed morphologically with a Zeiss 40 $\times$  water immersion lens (N.A. = 0.7). It was frequently necessary to reorient several times to examine all cells within the clone. After recording, a few embryos were fixed immediately and processed for biotinylated-dextran staining. We observed the remainder of the embryos up to 5 days of development. Because of limitations in our ability to continuously follow single cells, we limited these samples to clones with only the same cell shapes.

For observations by time-lapse videomicroscopy, single blastula cells were labeled with rhodamine-dextran. Single embryos were immobilized in 0.075% agarose between coverslips. At 50% epiboly, we recorded the deep cell layer, capturing five optical sections for both white light and epifluorescence every 90 seconds until early-somite stage. Cell fate was determined as described above.

### Microscopy and imaging

Observations were made on a Zeiss Axioskop equipped with a low-light camera (Newvicon VS2000N, Videoscope) and Intensifier (KS-1381, Videoscope). Imaging and data storage is described in Kane et al. (1996). Adobe Photoshop 4.0 was used to add pseudocolor and merge fluorescent and bright-field images.

### Production and purification of the Fkd2 antibody

The His-tag vector system (Qiagen) was used to express a fusion protein of dihydrofolate reductase and the N terminus of Fkd2. The following primers (F: 5'-GGTGATCAATTGAGGAAA-AAGCTGGG; R: 5'-AATGATCAGGATGCATTGAGGACAGA; Odenthal and Nüsslein-Volhard, 1998) were used to subclone the Fkd2 fragment into the PQE-16 vector. Rabbit Fkd2 antibodies were affinity-purified with Affi-Gel 15 beads (Bio-Rad). Specificity of purified antiserum was confirmed by immunoblotting.

### Whole-mount staining and sectioning

Embryos were staged and fixed overnight at 4°C in 4% buffered paraformaldehyde. Whole-mount antibody staining was performed as in Schulte-Merker et al. (1992) with the following modification: we frequently used 0.03% CoCl<sub>2</sub> in the DAB color reaction. The following antibodies were used: anti-Fkd2, anti-Ntl (Schulte-Merker et al., 1992), anti-Zn8 (Trevarrow et al., 1990). For sectioning, embryos were stained as whole mounts, dehydrated, embedded in Epon A12 and serially sectioned.

## RESULTS

### Zebrafish endodermal precursors originate at the blastoderm margin

To determine the origin of endoderm, we labeled single

marginal cells with lineage tracer dye in mid-blastula stage embryos when there were 1000 to 4000 cells present. The resulting small clone of cells was mapped relative to the blastoderm margin in the radially symmetrical blastoderm stage embryo (40% epiboly; Fig. 1A) and the dorsoventral location of the clone was subsequently determined an hour later in the early gastrula, following formation of the embryonic shield (the future dorsal midline; Fig. 1B). In order to learn the fate of these cells, we continued to follow their progeny in the embryo between 1 and 5 days of development (Fig. 1D-G).

The progeny of marginal clones differentiated into only endoderm, only mesoderm, or a combination of both derivatives. The fate map data is summarized in Fig. 2A-D,

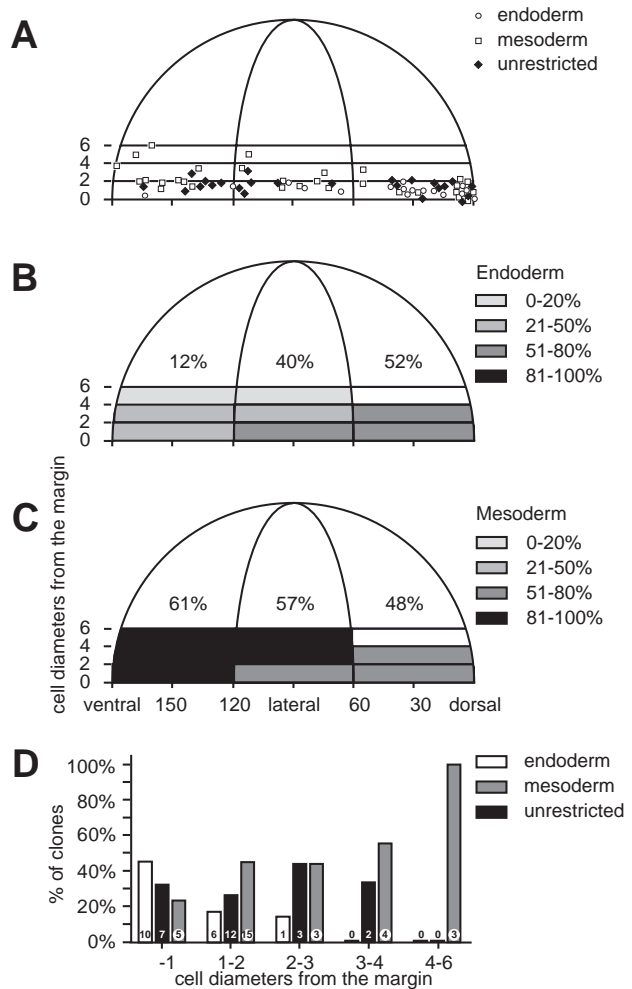


**Fig. 2.** Cells at the blastoderm margin generate endoderm and mesoderm. (A) Position of endodermal, mesodermal and unrestricted clones at 40% epiboly, as presented in Fig. 1C. (B-D) Summary data from our fate map clones illustrating location biases. The percentage of clones giving rise to endodermal derivatives (B) or mesodermal derivatives (C). The percentage of dorsal (0-60°), lateral (61-120°), and ventral (121-180°) clones which were restricted to a single germ layer is also indicated above a sector of the margin, this was calculated by dividing the number of clones giving rise exclusively to endoderm (or mesoderm) by the total number of clones that gave rise to endoderm (or mesoderm). (D) The percentage of endodermal, mesodermal and unrestricted clones in relation to distance from the blastoderm margin.

showing the blastoderm distribution of all the clones, the percentage of clones giving rise to endoderm or mesoderm, and the distribution of the clones as a percent with respect to distance from the margin. Of the 71 clones, 17 gave rise to endoderm only, 30 gave rise to mesoderm only, and 24 clones gave rise to derivatives of both mesoderm and endoderm. None of the clones gave rise to ectodermal precursors. To determine the overlap between involuting cells and noninvoluting cells, we labeled cells earlier, thus creating larger clones of 8 to 16 cells by 40% epiboly. Of these 14 clones, 4 gave rise to both mesoderm and ectoderm, 6 gave rise to both mesoderm and endoderm, and 4 gave rise to mesoderm only. No clones gave rise to both endoderm and ectoderm confirming the observation that there is a band of mesoderm separating the two fields.

Surprisingly, our fate map data set shows a marked density of clones in the dorsal half of the blastula. Also, dorsal clones are distributed closer to the margin than lateral or ventral clones. This is likely due to our labeling cells an hour before we mapped them (see Discussion) perhaps caused by a marked compaction of cells on the dorsal side of the embryo occurring between 30% and 40% epiboly (Warga and Nüsslein-Volhard, 1998).

At 40% epiboly, cells have not yet begun to involute to form the hypoblast. To determine where marginal clones mapped at 40% epiboly were later located at shield stage, we remapped a subset of the fate map data set ( $n=12$ ) with respect to the blastoderm margin. By shield stage, labeled cells frequently had involuted into the hypoblast (73%), and often these cells had migrated more than 6 cell diameters from the margin (53%). Thus, by shield stage, the majority of marginal cells have already involuted; many are no longer near the margin, but rather are located beneath the presumptive ectoderm.

Hence, endodermal precursors arise from cells primarily on the dorsal side, near the margin. While cells in this region also contribute to mesodermal structures, the majority of mesodermal precursors originate from cells on the ventral side and from dorsal cells located further from the margin. Among clones restricted to a single germ layer, dorsal clones tend to be endoderm and ventral clones tend to be mesoderm. Unrestricted clones originate from all positions along the dorsoventral margin,

decreasing with distance from the margin. Thus, while blastula cells are unrestricted to a particular germ layer, blastomeres closest to the margin on the dorsal side are biased toward endodermal fate.

### Organ precursors come from overlapping fate map fields

The progeny of marginal blastomeres contributed to all of the tissues classically thought to be endoderm (Fig. 1J-P). Although each organ derives from an extensive field of cells whose boundaries overlap with that of other organs, there is general correspondence for more anterior organs to map more dorsally and more posterior organs to map more laterally (Fig. 3A). Pharynx comes predominantly from more dorsal cells,

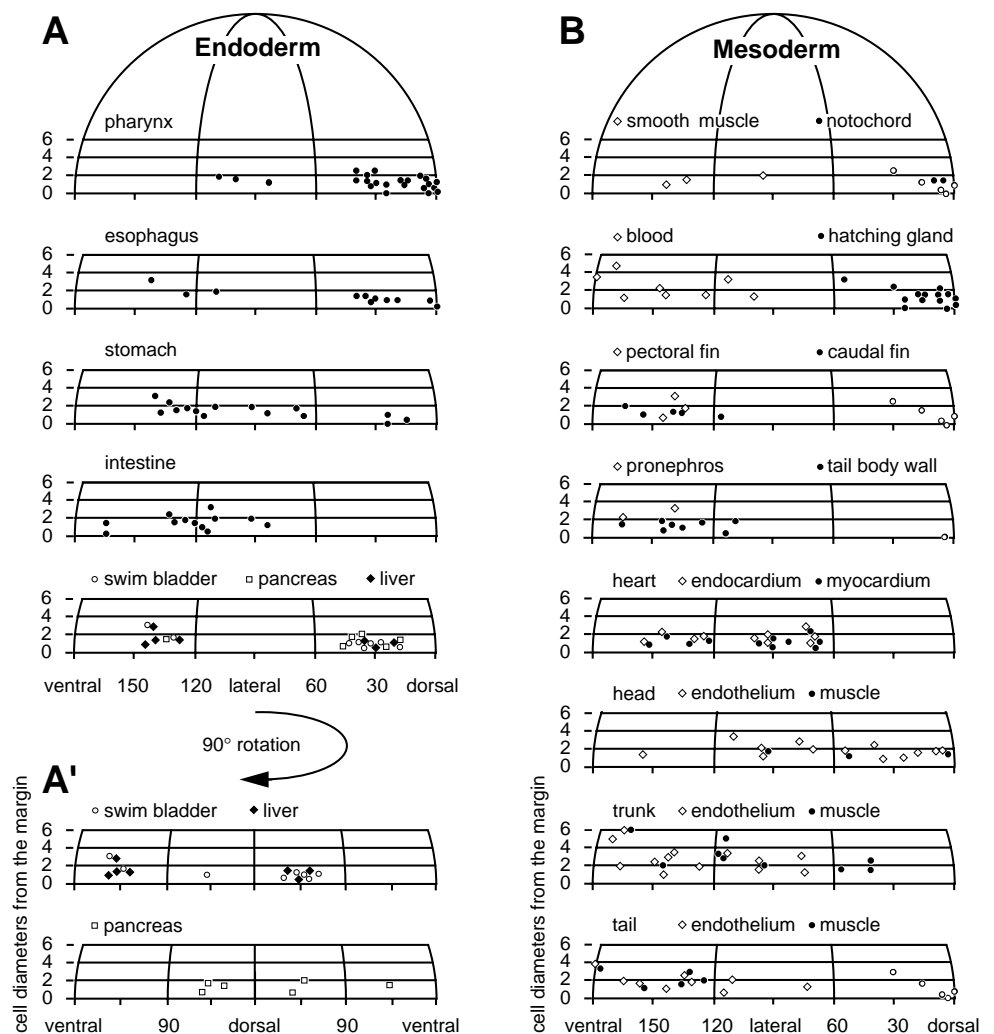


**Fig. 3.** Fate map positions of endodermal and mesodermal derivatives. The diagrams are as presented in Fig. 1C. (A) Endodermal derivatives. In the case of the liver, swimbladder and pancreas, we also present a rotated dorsal view (A'). (B) Mesodermal derivatives. In the case of notochord, caudal fin, tail body wall and tail muscle, a subset of these tissues were derived from marginal deep cells (black circle) or from a detached group of cells located at the margin known as the forerunner cells (white circles). Forerunner cells never involute and instead lead the margin during epiboly, ending up in the tailbud where they intermingle with ventrally derived cells (Melby et al., 1996; Cooper and D'Amico, 1996). Like endoderm, the anterior-posterior location of the endothelial blood vessels and muscle roughly corresponds to dorsoventral position in the late blastula, disregarding tail muscle derived from the forerunner cells.

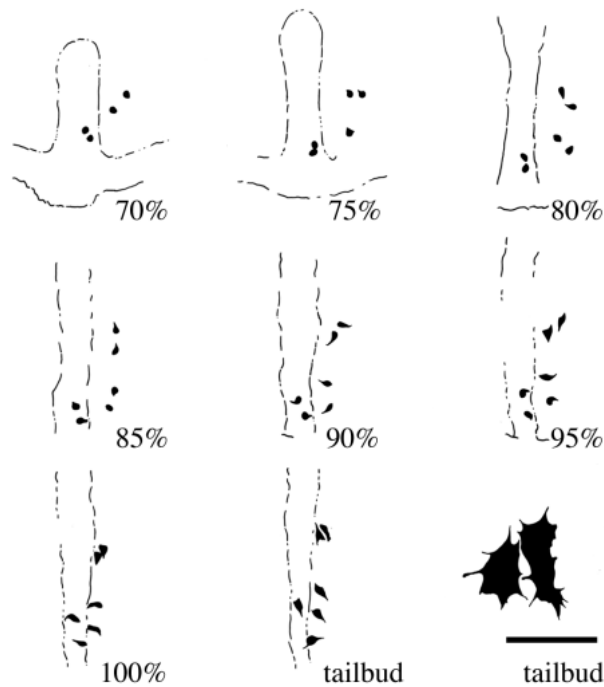


**Fig. 4.** Endodermal precursors acquire a characteristic morphology during gastrulation. Five marginal clones were followed by time-lapse videomicroscopy during gastrulation. Observation of the clones continued until 96 hours, by which time the clonal progeny had differentiated into identifiable derivatives (in this example: pharynx, esophagus, liver and swimbladder). Drawings were traced from selected frames of the time-lapse video. The embryonic axis is outlined with broken lines; the blastoderm margin is below and eventually moves out of the field. Initially all four involuted cells appear round. Beginning around 80% epiboly, the more anterior cells of the clone begin to flatten and acquire a tear drop shape. As cells continue to flatten they appear to enlarge. Higher magnification reveals the presence of numerous filopodia. Scale bar: 100  $\mu\text{m}$  for all except last panel, which is 25  $\mu\text{m}$ .

esophagus and stomach from more lateral cells, and intestine from more ventrolateral cells. Some of the organs, which are asymmetrically located in the adult, especially the liver and pancreas, exhibit a curious asymmetry in their fate map fields. The liver-swimbladder fields, together, come from two separate locations in the blastula, one almost exclusively on the right dorsolateral region and one on the left ventrolateral region (Fig. 3A'). An inverse, but slightly less consistent relationship, was found for clones generating pancreas.

Regardless of the considerable overlap in distributions of cells giving rise to different endodermal derivatives, precursors are not indiscriminately mingled with one another along the margin. Often there is a nonrandom association between precursors of different endodermal derivatives, which noticeably correlates with their arrangement along the gut. Thus, pharynx and esophagus commonly derive from single clones, likewise stomach and intestine (Table 1). However, the liver, swimbladder and pancreas, generally considered diverticula, or outpocketings of the gut wall, most often derive from clones that also gave rise to pharynx and esophagus, indicating a close relationship between these diverticula and more anterior tissues of the gut tract.

The progeny of marginal blastomeres were also found in many derivatives of the mesoderm (Fig. 3B). Notochord and hatching gland derive from dorsal clones, heart, blood and pronephros derive from ventral clones, while the precursors of muscle and endothelium of the blood vessels are spread throughout. These distributions are consistent with other zebrafish fate maps. We also identified the origin of two mesodermal tissues not previously mapped: smooth muscle surrounding the gut and pectoral fin mesenchyme, which consists of stellate mesenchymal cells, appearing similar to migratory cells described for the caudal fin in both zebrafish (Melby et al., 1996) and another teleost, the rosybarb (Wood and Thorogood, 1984).

Notably, the hypochord appeared in none of our clones. This peculiar tissue, consisting of a median row of cells beneath the notochord, has no obvious association with the gut, but is sometimes assigned to the endoderm. Our data show that hypochord is not derived from cells near the margin and implies perhaps that hypochord should not be considered endodermal.

#### Endoderm precursors acquire a unique cell morphology, depth and location after the onset of gastrulation

About one third of labeled blastula cells gave rise to derivatives of both germ layers, demonstrating that when they were labeled at the 1000- to 4000-cell stage, endoderm and mesoderm have not yet segregated from one another. Following labeled marginal cells by time-lapse videomicroscopy, we observed that differences arise between endodermal and mesodermal cells during gastrulation. Between 70% and 80% epiboly, some hypoblast cells begin to change their morphology. First adopting a tear-drop shape, these cells become increasingly flatter and lose their polar appearance. Additionally, they obtain filopodial processes (Fig. 4). In contrast, neighboring cells undergo minimal shape change, remaining spherical and lacking filopodia throughout gastrulation (compare Fig. 5A to C). We kept track of labeled hypoblast cells in the mid to late gastrula (16 embryos; Table 2) and determined their fates at a later stage (Fig. 5A-D). We found that flattened cells in all cases gave rise to endodermal tissues and round cells in all cases gave rise to mesodermal tissues. Thus, by late gastrulation, endoderm and mesoderm are distinguishable.

We determined the depth of flat and round cells relative to the yolk cell between 80% and 100% epiboly. Within the hypoblast, flattened cells were always internal, next to the yolk cell, while rounded cells were always more superficial (Table 2). We confirmed this observation by fixing, staining and sectioning five of these embryos immediately after recording the labeled cells (Fig. 5E-H). More careful examination of live embryos revealed that, by late gastrulation, flattened cells form a sparse, but regular monolayer (Fig. 5I), which is overlain by the more coherent multilayer of rounded cells (Fig. 5J).

Moreover, endodermal precursors are found in characteristic locations. During gastrulation, mesodermal and endodermal cells converge towards the dorsal midline and, in the process, distribute along the anterior-posterior axis (Fig. 6A-D). By late gastrulation endodermal precursors are distributed within the prechordal plate (the anterior dorsal hypoblast), and alongside the dorsal midline (Fig. 6C) in a distribution roughly resembling a triangle whose base encompasses an arc of roughly 150° (Fig. 6E), its apex

below the leading edge of the dorsal hypoblast where endodermal precursors are excluded, and only mesodermal hatching gland precursors are found (data not shown). Thus, by late gastrulation, endoderm has become a definitive germ layer, its cells possessing an unique cell shape and the cell layer itself having an unique depth and location in the embryo.

### Fkd2 is expressed in endodermal precursor cells

To more fully characterize endodermal development, we generated an antibody to the protein product of the zebrafish *fkd2* gene, a gene similar to mouse *HNF3 $\gamma$* . During development, *fkd2* mRNA is expressed throughout epiboly and gastrulation in the dorsal blastoderm, and later in the differentiating gut (Odenthal and Nüsslein-Volhard, 1998).

Using the Fkd2 antibody, we found that cells begin to express Fkd2 before and as they acquire endodermal characteristics. Zebrafish Fkd2 protein, which is nuclearly

localized, is first expressed at the onset of epiboly in presumptive dorsal cells, and in syncytial nuclei of the yolk cell (Fig. 7A). Expression in the yolk cell spreads rapidly around the margin and towards the animal pole while expression in the blastoderm remains restricted to cells which become the embryonic shield. Around 60% epiboly, we first detect a lateral subset of sparsely distributed cells within the hypoblast, which based on their location and comparison with subsequent stages, we determined to be endodermal precursors (Fig. 7B; arrow). By 90% epiboly, prechordal plate (anteriorly) and notochord (posteriorly) have differentiated from within the dorsal hypoblast; both tissues express Fkd2, as does the presumptive floor plate of the nervous system (Fig. 7C). Likewise cells in the lateral hypoblast (arrow) form a pattern resembling the spatial distribution of late gastrula endodermal precursors (Fig. 6E). Based on their characteristic cell shape, these lateral cells, along with the deeper cells in the prechordal

**Fig. 5.** Endodermal precursors occupy a stereotypic depth in the hypoblast. (A) Flattened cells, characteristic of the endodermal precursors in the late gastrula; note faint filopodia (arrows). At 100% epiboly, these cells were located directly adjacent to the yolk cell. (B) By 96 hours, these cells had differentiated into swimbladder tissue (sb) neighboring the stomach (st). (C) Rounded cells, characteristic of mesodermal precursors in the late gastrula; note lack of filopodia, however some cells show protrusive activity (arrow). At 90% epiboly, these cells were intermingled within a coherent layer of unlabeled cells of similar morphology one cell diameter up from the yolk cell. (D) By 30 hours, these cells had differentiated into paraxial muscle and 1 endothelial cell (arrow). (E-H) Five clones were examined at 90% epiboly and then immediately fixed, stained and sectioned. Illustrated is one example. The clone in the live embryo, deep (E) and superficial (F) planes of focus. Cells *a*, *b* and *e* are large and flattened endodermal precursors; one of several filopodia on cell *a* is indicated (arrow). Cells *c* and *d* are smaller and rounder mesodermal precursors, note cell *c* partially overlies cell *a*. (G) The same cohort of cells in the whole-mount preparation; note the filopodia on cell *a* (arrow). (H) Transverse section (10  $\mu$ m) through cells *a*, *c*, *d*, and *e*. Both cell *a* and *e* are in the deepest hypoblast cell layer, beneath cells *c* and *d*. The extremities of cell *a* and *e* are indicated with arrowheads and an arrow, which further indicates the filopodia on cell *a*. (I,J) Unlabeled cells in the live embryo at 100% epiboly. The field of view is located 45° away from the dorsal midline near the level of the equator, because the embryo is spherical, cells at the bottom of the field are in a deeper plane of focus than cells at the top. (I) Deep plane of focus, six endodermal precursor cells (indicated with numerals) – each cell spaced roughly one cell diameter apart from one another – overlay the yolk cell whose nuclei (n) are also in focus. Filopodia (arrows) on cell 1 are indicated. (J) Superficial plane of focus, a layer of mesodermal precursor cells lie above the endodermal cells. Mesodermal precursor cells form a coherent layer – there are no spaces between cells. Asterisk denotes the positions of the underlying endoderm cells. Notice cells 1, 4 and 5 are partially visible. Scale bar: 10  $\mu$ m (A,C, E-G, and I,J), 50  $\mu$ m (B,D), 5  $\mu$ m (H).

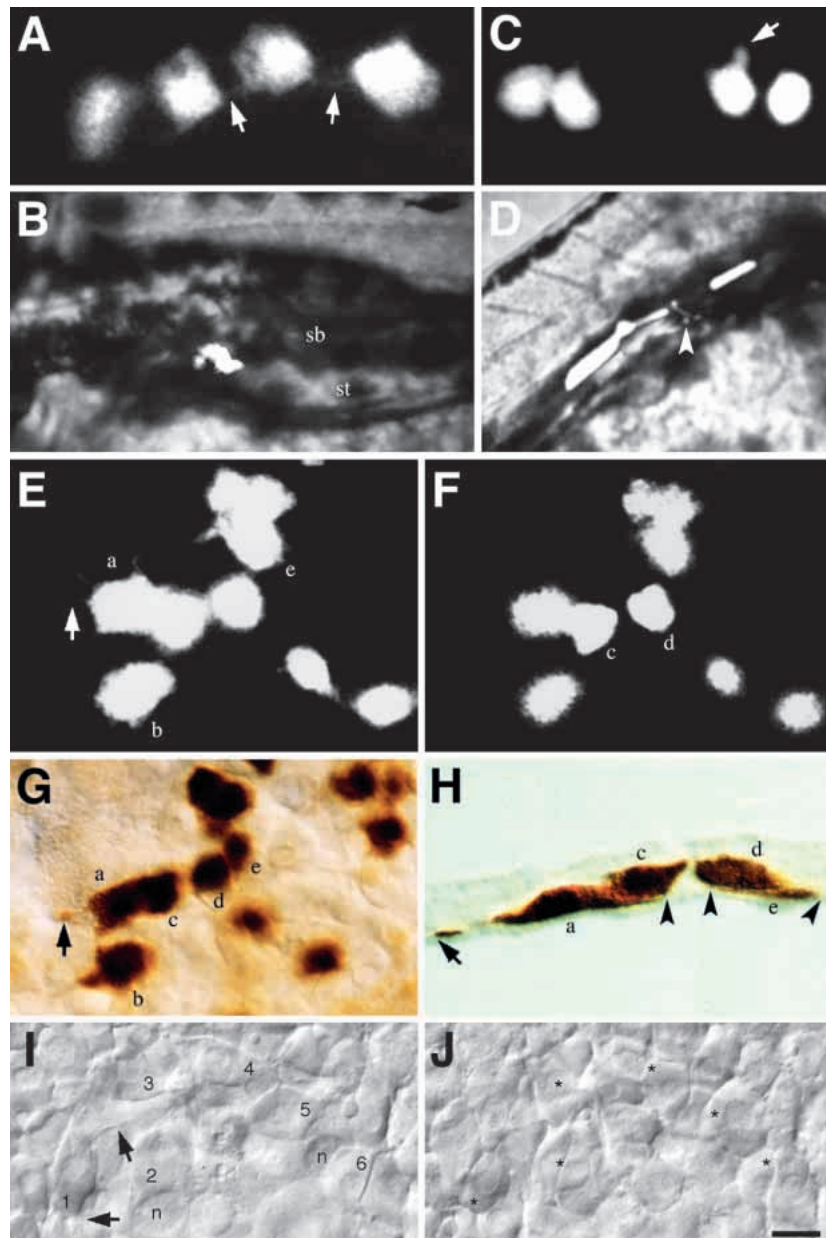


**Table 1. Clonal relationship between different endodermal tissues**

	hatching gland (14)	pharynx (23)	esophagus (11)	swim bladder (8)	liver (7)	pancreas (6)	stomach (15)	intestine (12)
hatching gland	–	6	0	0	0	0	1	0
pharynx	6	–	8	5	3	3	4	2
esophagus	0	8	–	7	5	3	4	2
swim bladder	0	5	7	–	5	3	3	1
liver	0	3	5	5	–	1	3	1
pancreas	0	3	3	3	1	–	2	1
stomach	1	4	4	3	3	2	–	11
intestine	0	2	2	1	1	1	11	–

Intersection of a row and column indicates the number of clones containing both tissues. Numbers in parenthesis indicate the total number of clones giving rise to each tissue. Hatching gland is included because it is not clearly assigned to the mesoderm. Both the hatching gland and pharynx derive from the anterior prechordal plate and differentiate in very close proximity to one another thus, explaining their clonal relatedness. Shading indicates percentage that two tissues share a common precursor (denominator is based on the least represented tissue). Clear cells 0%, lightly shaded 7-20%, medium shaded cells 21-50%, darkly shaded cells 51-100%.

plate, are endodermal precursors (Fig. 7D). In agreement with this interpretation, these Fkd2-positive cells form a discernible monolayer above the yolk cell (Fig. 7E). Through later development, Fkd2 protein expression becomes increasingly restricted to endodermal cells along the differentiating gut (Fig. 7F,G), progressively disappearing from dorsal mesodermal and ectodermal tissues. Then, at 1 day, Fkd2 protein becomes difficult to visualize although *fkd2* mRNA continues to be expressed throughout the differentiating gut.

### Loss of *cyclops* gene function results in a reduction of endodermal and mesodermal precursors

In both mouse and chick, signals from the prechordal plate control the expression of genes necessary for neural plate patterning (Ang et al., 1994; Shimamura and Rubenstein, 1997; Storey et al., 1995). As we have shown above in the zebrafish, endoderm as well as mesoderm derives from the prechordal plate. For this reason, we examined a mutation in *cyclops*, a gene that is required for normal cell fate of the neuroectoderm, particularly the forebrain and the floor plate of the spinal cord (Hatta et al., 1991, 1994; Strähle et al., 1993). We found that, in *cyclops*-mutant embryos, pharyngeal endoderm is reduced: the pharyngeal pouches are smaller and occasionally more anterior pouches are absent (Fig. 8A,B).

Examination of mutant embryos at 90% epiboly revealed normal looking endodermal precursors in the prechordal plate (Fig. 8C,D), but the prechordal plate was markedly thinner (Fig. 8E,F). Embryos sorted by this phenotype and then assayed by Fkd2 antibody staining had about 50% fewer positive cells in the prechordal plate (Fig. 8I,J) including cells that we have shown to be endodermal precursors (Fig. 8K,L). These results

**Table 2. The morphology and depth of cells in the hypoblast predicts endodermal or mesodermal fate**

Morphology*	Embryo	Number‡	Depth§	Fate
Flattened	205	8	ND	Endoderm
	170	6	1	Endoderm
	178	5	1	Endoderm
	226b	2	1	Endoderm
	165	2	1	Endoerm
	226a	4	1	Endoderm
	154	6	1	Endoderm
	164a	9	1	Endoderm
	164b	2	1	Endoderm
	192	4	1	Endoderm
	152	4	ND	Endoderm
Round	176a	4	2	Mesoderm
	176b	6	2	Mesoderm
	207	10	ND	Mesoderm
	216	8	ND	Mesoderm
	184	6	2&3	Mesoderm

\*Using a 40× water immersion lens, we examined embryos at intervals between 70% and 100% epiboly, recording cellular morphology of the entire clone. Observation of labeled cells continued until they differentiated into a tissue, which in the case of endoderm was always by 5 days. Only clones having a similar cell morphology were followed to avoid ambiguity about later cell fate.

‡Number of cells in the clone.

§Cell depth was determined by counting cell layer up from the yolk cell. We classified depth 1 as the layer immediately above the yolk cell. ND, not determined.

concur with a previous study showing that the expression of the dorsal mesodermal marker *gooseoid* is reduced in the prechordal plate of *cyclops*-mutant embryos (Thisse et al., 1994).

The prechordal plate is derived from dorsally located marginal cells. As cells in this location, in addition to endodermal pharynx, give rise to mesodermal derivatives such as notochord and hatching gland, we asked if mesodermal tissues were similarly depleted in *cyclops* mutants. We found fewer Fkd2-positive cells present in the leading edge of the prechordal plate, which expresses Fkd2 more intensely (Fig. 8G,H). Likewise, hatching gland, its mesodermal derivative, was diminished (wt: 259±37 cells, *n*=16; *cyclops*: 154±27 cells, *n*=16). Unexpectedly, the notochord, which appears relatively normal in 1-day-old mutants, also had fewer positive cells (Fig. 8I,J,M,N). In total, many of the structures derived from the dorsal margin were diminished, regardless of whether they were endoderm or mesoderm.

## DISCUSSION

### The endodermal tissues derive from the dorsal and lateral blastoderm margin

Endoderm in zebrafish originates from a narrow field of cells along the margin of the blastoderm embryo. Most endodermal precursors are located within 2 cell diameters from the blastoderm margin and no precursors were found more than 4 cell diameters from the margin. Along this territory, the anlagen of endodermal organs are stretched out in broadly overlapping fields, and are roughly distributed from dorsal to ventral according to their later arrangement along the anterior-

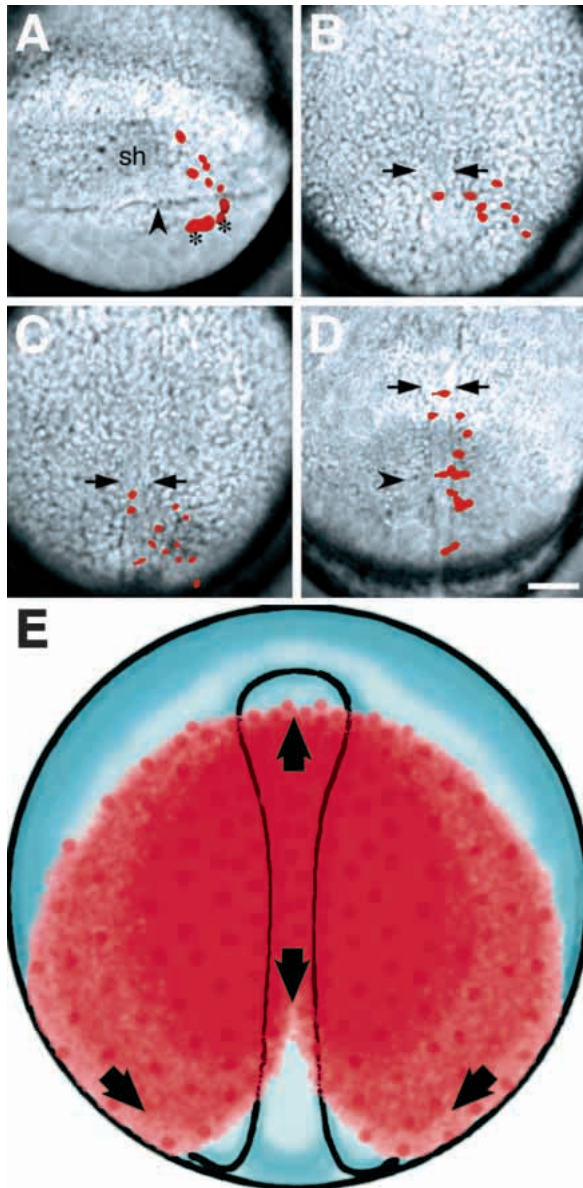


**Fig. 6.** Endodermal precursors are stereotypically distributed in the late gastrula. (A-D) Illustrate the convergence of endodermal precursors towards the dorsal midline from selected composite frames of a time-lapse video. Labeled cells are pseudocolored red. (A) The clone at shield stage, consisting of six deep cells and four enveloping layer cells (asterisks), to the right of the embryonic shield (sh). The labeled deep cells have already involuted deep into the hypoblast; arrowhead, blastoderm margin. (B) By 80% epiboly, labeled cells have begun to converge towards the embryonic axis whose boundaries are indicated with arrows for this and subsequent panels. (C) By 100% epiboly, labeled cells have begun to spread towards the animal pole. (D) At the 4-somite stage, the labeled cells now extend anterior-posteriorly along the axis. The more anterior cells were in the prechordal plate and gave rise to pharynx, a common prechordal plate derivative in our data set, the more posterior cells gave rise to liver, swimbladder and stomach; arrowhead, first somite furrow. (E) Illustrates the spatial distribution of endodermal precursors in the late gastrula based on our data. Red indicates where cells of the endoderm were observed, and arrows indicate directions cells move to meet at the dorsal midline and spread antero-posteriorly. Scale bar: 100  $\mu$ m.

posterior axis of the embryo. What with no endodermal structures in the tail, few endodermal precursors originate on the ventral side of the blastula. Thus, endoderm is derived predominantly from the dorsal and lateral regions of the blastoderm margin, whose cells come to be located along the midline of the embryo.

Whereas endodermal precursors are located exclusively at the margin before gastrulation begins, by the shield stage, the majority of cells giving rise to endoderm are located far from the margin deep in the newly formed hypoblast. This implies that endodermal precursors are among the earliest involuting cells and are unlikely to derive from regions that also give rise to ectodermal precursors. This is in agreement with our findings that endoderm and ectoderm never derive together from single clones established between the 1000- to 4000-cell stages.

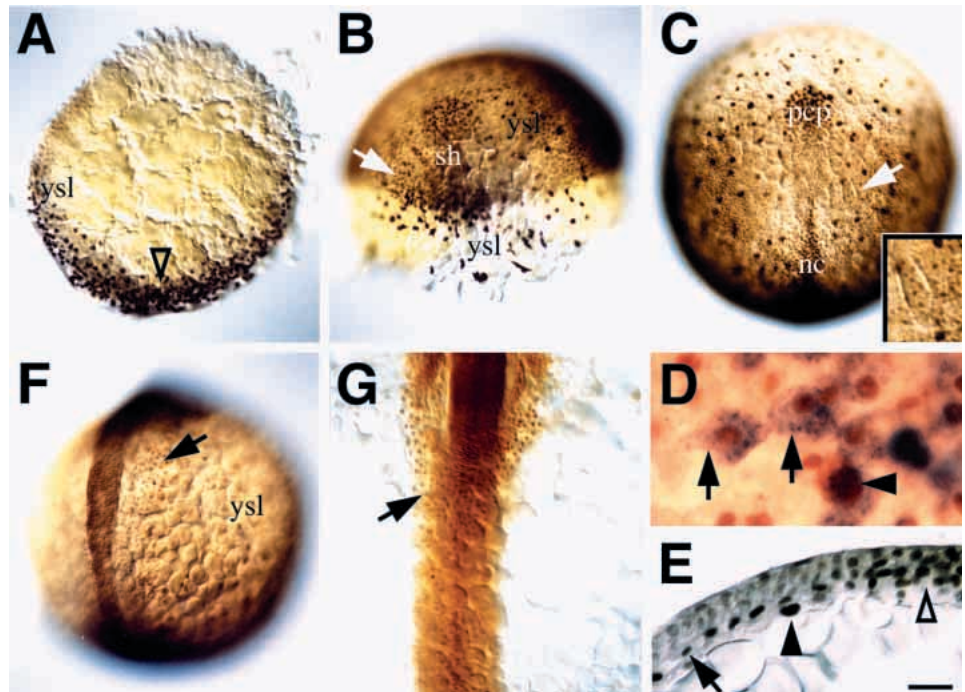
One of our more unexpected observations is that more clones are found dorsally than ventrally (Fig. 2A). Re-evaluating the fate maps by Kimmel et al. (1990; Figs 5, 7), we see a similar asymmetric distribution in their enveloping layer and deep cell fate maps: twice as many clones are found dorsally. Since both fate maps were made by labeling cells blindly before the dorsal side is apparent, we would expect labeled clones to be randomly located. Furthermore, there is no obvious way that we have biased our data, for example, by discarding boring ventral clones because they made little endoderm. Thus, between the labeling of cells, at the mid blastula, and the mapping of cells, at 40% epiboly and shield stage, cells must move dorsally. The period of displacement correlates with the timing of a noticeable compaction of cells on the dorsal side of the embryo, which draws dorsal cells closer to the midline and closer towards the margin between 30% and 40% epiboly (Warga and Nüsslein-Volhard, 1998).

#### Marginal cells give rise to both endodermal and mesodermal precursors

In addition to endodermal derivatives, we found that clones of cells derived from marginal blastomeres gave rise to a number of mesodermal derivatives. Many blastomeres were not restricted in the 2000-cell blastula, as a third of the clones produced derivatives of both germ layers. Thus, in the mid blastula between the 1000- and 4000-cell stage, different fates have not yet separated. In past studies, we have observed cells shortly before involuting to divide and give rise to both an endodermal and mesodermal precursor (Warga and Kimmel, 1990; Fig. 7B) suggesting that even as late as 40% epiboly, at least some cells are still bi-potent. Thus, the apparent intermingling of restricted endodermal and mesodermal clones in our fate map probably reflects a mix of partially unspecified cells.

Our fate map most resembles the previous zebrafish fate maps of Kimmel et al. (1990) and Melby et al. (1996). The map by Kimmel et al. was made by similar methods to ours. The significant difference is that we find precursors of endoderm and mesoderm greatly intermingled, while they show mesodermal precursors more distantly located from the margin. Because our map has notably more endoderm and considerably more data points near the margin, the difference is very likely due to our focusing specifically on the blastoderm margin. The map by Melby et al. (1996) corresponds with ours in terms of mesodermal precursors, but does not describe any endodermal precursors. Because the Melby map was made at the shield stage, when we found that most of our clones had

**Fig. 7.** Fkd2 protein is an early marker of endodermal precursors. (A) Dome stage, animal pole view; presumptive dorsal side (open arrowhead). (B) 60% epiboly, dorsal oblique view; presumptive endoderm precursor cells in focus on the left side (arrow) and larger, more irregular-shaped yolk syncytial nuclei in focus on the right side. (C) 90% epiboly, dorsal view; the lateral wing of endoderm precursor cells (arrow). Inset is a closeup of this location showing smaller endoderm nuclei, and larger yolk cell nuclei. (D) 90% epiboly, higher magnification showing characteristic endoderm precursor cells (arrows) labeled *in vivo* with fixable lineage tracer and then fixed and stained for the tracer (blue) and Fkd2 immunoreactivity (brown); 23 cells were analyzed in this manner. Arrowhead indicates a Fkd2-positive yolk cell nucleus. (E) 90% epiboly, transverse section (10  $\mu$ m) through the midline (open arrowhead), showing one of several cell nuclei in the endodermal layer (arrow) and an underlying yolk cell nucleus (arrowhead). (F) 10-somite stage, dorsal oblique view; endodermal cells in focus on the right side (arrow). (G) 18-somite stage, dorsal view; endodermal cell sheet (arrow) in midline. Scale bar: 100  $\mu$ m (A-C, F), 50  $\mu$ m (G, and inset C), 20  $\mu$ m (E), 10  $\mu$ m (D); abbreviations: nc, notochord; pcp, prechordal plate; sh, shield; ysl, yolk syncytial nuclei.



involved deep into the hypoblast (Fig. 6A), endodermal precursors could not be easily labeled.

Often we found that more than one endodermal derivative descended from a single marginal cell. However, the tendency for tissues to be clonally related was nonrandom: generally, neighboring tissues were clonally related, for example pharynx and esophagus frequently descended from common clones.

In higher vertebrates, the liver and pancreas are derived from evaginations of the gut near the caudal end of the stomach (Patten, 1951). We find that the precursors of the liver and pancreas are more closely related to precursors of the pharynx and esophagus than the stomach. This data supports the view that the teleost and tetrapod stomachs may not be homologous (Harder, 1975) but rather that the zebrafish stomach may be homologous to the anterior intestine of higher vertebrates.

Regarding these diverticula, we found asymmetric locations for the blastula progenitors of the liver, swimbladder and pancreas. While this implies no asymmetry of the blastula, it does suggest that the morphogenetic processes that follow are asymmetric. Thus, small groups of progenitor cells which come from asymmetric positions unite to form a single tissue, suggesting that the liver, swimbladder and pancreas developmental fields must span the midline of the embryo. Since the dorsoventral blastula fate map translates into an anterior-posterior map in the embryo, perhaps the point at which the fate map switches sides may correlate to the location that the derived field intersects the midline.

### The endodermal germ layer emerges during gastrulation

We have observed no molecular or morphological differences between presumptive endodermal and mesodermal cells before gastrulation (Warga and Kimmel, 1990; R. M. W., unpublished

data). However, beginning at about 75% epiboly, at the time when cells become irreversibly committed to either epiblast- or hypoblast-derived fate (Ho and Kimmel, 1993), a population of hypoblast cells segregate and characteristically flatten. These cells make up a noncontiguous single cell layer deep in the embryo against the yolk, are characteristically distributed alongside the midline, and their progeny will contribute exclusively to endodermal organs. Other more rounded and superficial cells in the hypoblast do not contribute to endoderm, but instead become mesoderm.

Thus, we hypothesize a hierarchical sequence of determinative events whereby a cell is first specified to either the epiblast or hypoblast and, subsequently, within the hypoblast, a specification to either the endoderm or mesoderm. Before this latter separation, cells appear to be an uniform population of migrating cells, and we see no distinguishing characteristics between the endodermal and mesodermal precursors. The intermingling of endodermal and mesodermal precursors in our fate map is in agreement with this hypothesis. Additional support comes from our finding that, in *cyclops*-mutant embryos, irrespective of germ layers, dorsally derived endodermal and mesodermal structures (both precursors and derivatives) are reduced. As *cyclops* has been cloned and shown to be expressed in all marginal cells before the onset of gastrulation (Rebagliati et al., 1998; Sampath et al., 1998), we infer from our data that *cyclops* gene activity, must be required prior to the formation of the endodermal and mesodermal germ layers.

In most vertebrates, endoderm emerges from a field of mixed mesodermal and endodermal precursors (*amphibians*: Pasteels, 1942; Lundmark, 1986; Purcell and Keller, 1993; Delarue et al., 1994; Minsuk and Keller, 1996; *sturgeon*: Bolker, 1993; *mouse*: Sulik et al., 1994). A recent re-evaluation argues that this is the case for *Xenopus* as well, where it seems that mesoderm does

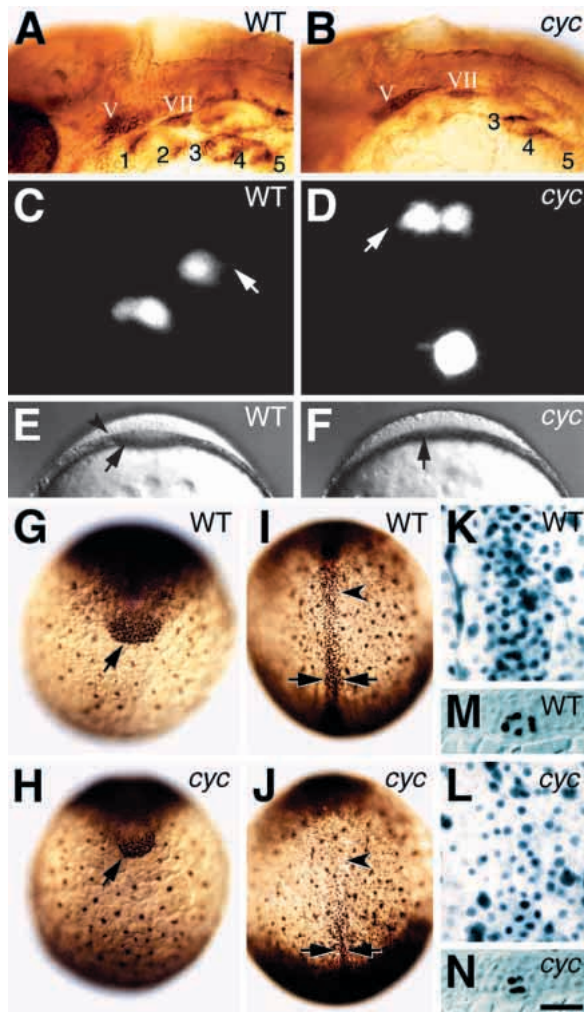


**Fig. 8.** Embryos mutant for *cyclops* have fewer dorsal endodermal and mesodermal precursors. (A,B) 30 hour embryos, side view, labeled with Zn8 antibody. The antibody labels the cell surfaces of the pharyngeal pouches (indicated by numerals 1-5) and sensory neurons in the cranial ganglia. (C,D) 100% epiboly, dorsal view; endodermal precursor cells in the prechordal plate of live embryos appear similar in both wild-type and mutant; arrows, filopodia. The very round and intensely bright cell in the lower field in D is preparing to divide and did so immediately after this image was captured. Progeny of both clones later gave rise to pharyngeal endoderm. (E,F) 90% epiboly, front view; the prechordal plate (arrow) is noticeably thinner in mutant embryos, and lacks a visible lateral boundary (arrowhead). (G-J) 100% epiboly stage embryos labeled with anti-Fkd2 illustrating the anterior prechordal plate (arrow); the posterior prechordal plate (arrowhead); and the notochord (between arrows). (K,L) Higher magnification of embryos (I,J) showing the endodermal precursors in a deep plane of focus. The boundary between prechordal plate endoderm and notochord, obvious in the *cyclops* embryo, is towards the lower field. (M,N) 100% epiboly stage embryos labeled with anti-Ntl, a notochord-specific marker. Shown is a transverse section (10  $\mu$ m) mid-trunk through the embryo. Using a 40 $\times$  lens, we counted all the intensely labeled Fkd2-positive nuclei in the anterior prechordal plate (wt: median = 195,  $n=3$ ; *cyclops*: median = 106,  $n=3$ ). Similarly, we counted all labeled nuclei in a 100 $\times$ 100  $\mu$ m field of the posterior prechordal plate (wt: median = 409,  $n=3$ ; *cyclops*: median = 210,  $n=3$ ) and the notochord (wt: median = 217,  $n=3$ ; *cyclops*: median = 120,  $n=3$ ). Endodermal precursors, labeled nuclei adjacent to the yolk, comprise a subset of the prechordal plate field (wt: median = 127,  $n=3$ ; *cyclops*: median = 60,  $n=3$ ). Scale bar: 100  $\mu$ m (A,B, E,F and G,H), 25  $\mu$ m (K,L), 8  $\mu$ m (C,D); abbreviations: V, trigeminal ganglion; VII, facial ganglion.

not originate solely from the deeper cells of the marginal zone, but also from cells in the superficial layer, which have been thought to only give rise to endoderm (Minsuk and Keller, 1997). After ingressing together into a single deep layer, it is observed that endodermal and mesodermal precursors subsequently separate into their respective germ layers.

In zebrafish, as the endoderm is sorted out from the mesoderm, we hypothesize that there may be a role for the yolk cell as a source of inductive signals for endoderm formation. While most cells of the zebrafish hypoblast have transient connections to the yolk cell, only the endoderm remains in continuous contact with the yolk cell throughout later gastrulation. In *Drosophila*, *fork head* is required for early gut differentiation (Weigel et al., 1989). Notably, in the zebrafish, syncytial nuclei of the yolk nearest the margin are one of the earliest populations to express Fkd2 protein (Fig. 7A). Shortly before zebrafish endodermal cells can be morphologically distinguished they too begin expressing Fkd2 (Fig. 7B). Given the close proximity of the endoderm to the yolk cell both before and after involution, the yolk cell is a likely source of signals for specification of endoderm. Indeed, the yolk cell has been shown to be a source of signals for dorsoventral patterning in trout (Long, 1983). The role that the yolk cell plays in the formation of zebrafish endoderm may shed light on the role of

the amphibian yolky vegetal cells or the mouse visceral endoderm, both of which may provide developmental functions homologous to that of the fish yolk cell.

This work was enriched by many discussions with Bess Melby and Don Kane. We thank Bess Melby, Don Kane, Bob Fleming, Lynne Angerer and the three anonymous referees, especially referee no. 1, for reading and commenting on early versions of the manuscript; Jörg Odenthal for generously providing the *fkd2* clone from which the antibody was generated; Matthias Hammerschmidt, Andreas Bergmann, Jörg Odenthal and Christine Stella for advice on antibody production; Stefan Schulte-Merker and Bill Trevarrow for antibodies; Ruth BreMiller and Heinz Schwarz for help with histochemistry. R. M. W. wishes to especially thank Peter O' Day and the late Dave Brumbley for help in learning electrophysiology, Larry Tabak for patience while writing this manuscript, and Bess Melby and Don Kane for their unflagging support. This work forms part of a Ph.D. dissertation submitted by R. M. W. to the Eberhard-Karls-Universität Tübingen, and was supported in part by a Max-Planck fellowship to R. M. W.

This paper is dedicated to the memory of Nigel Holder.

## REFERENCES

- Ang, S. L., Wierda, A., Wong, D., Stevens, K. A., Cascio, S., Rossant, J. and Zaret, K. S. (1993). The formation and maintenance of the definitive endoderm lineage in the mouse: involvement of HNF-3/forkhead proteins. *Development* **119**, 1301-1315.
- Ang, S. L., Conlon, R. A., Jin, O. and Rossant, J. (1994). Negative signals from the mesoderm regulate the expression of mouse *otx2* in ectoderm explants. *Development* **120**, 2979-2989.
- Bolker, J. A. (1993). Gastrulation and mesoderm morphogenesis in the white sturgeon. *J. Exp. Zool.* **266**, 116-131.
- Cooper, M. S. and D'Amico, L. A. (1996). A cluster of noninvoluting endocytic cells at the margin of the zebrafish blastoderm marks the site of embryonic shield formation. *Dev. Biol.* **180** 184-198.

- Delarue, M., Sanchez, S., Johnson, K. E., Darribere, T. and Boucaut, J. - C. (1992). A fate map of superficial and deep circumblastoporal cells in the early gastrula of *Pleurodeles waltl*. *Development* **114**, 135-146.
- Delarue, M., Johnson, E. E. and Boucaut, J.-C. (1994). Superficial cells in the early gastrula of *Rana pipiens* contribute to mesodermal derivatives. *Dev. Biol.* **165**, 702-715.
- Dirksen, M. L. and Jamrich, M. (1995). Differential expression of *fork head* genes during early *Xenopus* and zebrafish development. *Dev. Genet.* **17**, 107-118.
- Dufort, D., Schwartz, L., Harpal, K. and Rossant, R. (1998). The transcription factor HNF3 $\beta$  is required in visceral endoderm for normal primitive streak morphogenesis. *Development* **125**, 3015-3025.
- Hammerschmidt, M. and Nüsslein-Volhard, C. (1993). The expression of a zebrafish gene homologous to *Drosophila* *snail* suggests a conserved function in invertebrate and vertebrate gastrulation. *Development* **119**, 1107-1118.
- Harder, W. (1975). *Anatomy of Fishes*. E. Schweizerbart'sche Verlagsbuchhandlung (Nägele und Overmiller), Stuttgart.
- Hatada, Y. and Stern, C. D. (1994). A fate map of the epiblast of the early chick embryo. *Development* **120**, 2879-2889.
- Hatta, K., Kimmel, C. B., Ho, R. K. and Walker, C. (1991). The *cyclops* mutation blocks specification of the floor plate of the zebrafish central nervous system. *Nature* **350**, 339-341.
- Hatta, K., Püschel, A. W. and Kimmel, C. B. (1994). Midline signalling in the primordium of the zebrafish anterior central nervous system. *Proc. Natl. Acad. Sci.* **91**, 2061-2065.
- Henry, G. L., Brivanlou, I. H., Kessler, D. S., Hemmati-Brivanlou, A. and Melton, D. A. (1996). TGF- $\beta$  signals and a prepattern in *Xenopus laevis* endodermal development. *Development* **122**, 1007-1015.
- Henry, G. L. and Melton, D. A. (1998). *Mixer*, a homeobox gene required for endoderm development. *Science* **281**, 91-96.
- Ho, R. K. and Kimmel, C. B. (1993). Commitment of cell fate in the early zebrafish embryo. *Science* **261**, 109-111.
- Hudson, C., Clements, D., Friday, R. V., Stott, D. and Woodland, H. R. (1998). *Xsox17* alpha and -beta mediate endoderm formation in *Xenopus*. *Cell* **91**, 397-405.
- Kane, D. A., Hammerschmidt, M., Mullins, M. C., Maischein, H.-M., Brand, M., van Eeden, F. J. M., Furutani-Seiki, M., Granato, M., Haffter, P., Heisenberg, C.-P., Jiang, Y.-J., Kelsh, R. N., Odenthal, J., Warga, R. M. and Nüsslein-Volhard, C. (1996). The zebrafish epiboly mutants. *Development* **123**, 47-55.
- Keller, R. E. (1975). Vital dye mapping of the gastrula and neurula of *Xenopus laevis*. I. Prospective areas and morphogenetic movements of the superficial layer. *Dev. Biol.* **42**, 222-241.
- Keller, R. E. (1976). Vital dye mapping of the gastrula and neurula of *Xenopus laevis*. II. Prospective areas and morphogenetic movements in the deep region. *Dev. Biol.* **51**, 118-137.
- Kimmel, C. B., Warga, R. M. and Schilling, T. F. (1990). Origin and organization of the zebrafish fate map. *Development* **108**, 581-594.
- Kimmel, C. B., Ballard, W. W., Kimmel, S. R., Ullmann, B. and Schilling, T. F. (1995). Stages of embryonic development of the zebrafish. *Dev. Dyn.* **203**, 253-310.
- Lawson, K. A., Meneses, J. J. and Pedersen, R. A. (1991). Clonal analysis of epiblast fate during germ layer formation in the mouse embryo. *Development* **113**, 891-991.
- Lee, R. K., Stainier, D. Y. R. and Fishman, M. C. (1994). Cardiovascular development in the zebrafish. II. Endocardial progenitors are sequestered within the heart field. *Development* **120**, 3361-3366.
- Lemaire, P., Darras, S., Caillol, D. and Kodjabachian, L. (1998). A role for the vegetally expressed *Xenopus* gene *Mix.1* in endoderm formation and in the restriction of mesoderm to the marginal zone. *Development* **125**, 2371-2380.
- Long, W. L. (1983). The role of the yolk syncytial layer in determination of the plane of bilateral symmetry in the rainbow trout, *Salmo gairdneri* Richardson. *J. Exp. Zool.* **228**, 91-97.
- Lundmark, C. (1986). Role of bilateral zones of ingressing superficial cells during gastrulation of *Ambystoma mexicanum*. *J. Embryol. Exp. Morph.* **97**, 47-62.
- Melby, A. E., Warga, R. M. and Kimmel, C. B. (1996). Specification of cell fates at the dorsal margin of the zebrafish gastrula. *Development* **122**, 2225-2237.
- Minsuk, S. B. and Keller, R. E. (1996). Dorsal mesoderm has a dual origin and forms by a novel mechanism in *Hymenochirus*, a relative of *Xenopus*. *Dev. Biol.* **174**, 92-103.
- Minsuk, S. B. and Keller, R. E. (1997). Surface mesoderm in *Xenopus*: a revision of the stage 10 fate map. *Dev. Genes Evol.* **207**, 389-401.
- Monaghan, A. P., Kaestner, K. H., Grau, E. and Schütz, G. (1993). Postimplantation expression patterns indicate a role for the mouse *forkhead/HNF-3 $\alpha$* ,  $\beta$ , and  $\gamma$  genes in determination of the definitive endoderm, chordamesoderm and neuroectoderm. *Development* **119**, 567-578.
- Nascone, N. and Marcola, M. (1995). An inductive role for the endoderm in *Xenopus* cardiogenesis. *Development* **121**, 515-523.
- Nieuwkoop, P. D. (1969). The formation of mesoderm in urodelean amphibians. I. The induction by the endoderm. *Roux's Arch. EntwMech. Org.* **162**, 341-373.
- Odenthal, J. and Nüsslein-Volhard, C. (1998). *fork head* domain genes in zebrafish. *Dev. Genes Evol.* **208**, 245-258.
- Pasteels, J. (1942). New observations concerning the maps of presumptive areas of the young amphibian gastrula (*Amblystoma* and *Discoglossus*). *J. Exp. Zool.* **89**, 255-281.
- Papaioannou, V. E. and Silver, L. M. (1998). The T-box family. *BioEssays* **20**, 9-19.
- Patten, B. M. (1951). *Early Embryology of the Chick*. New York: McGraw-Hill Book Company, Inc.
- Purcell, S. M. and Keller, R. E. (1993). A different type of amphibian mesoderm morphogenesis in *Ceratophrys ornata*. *Development* **117**, 307-317.
- Rebagliati, M. R., Toyama, R., Haffter, P. and Dawid, I. B. (1998). *cyclops* encodes a nodal related factor involved in midline signalling. *Proc. Nat. Acad. Sci. USA* **95**, 9932-9937.
- Sampath, K., Rubinstein, A. L., Cheng, A. H. S., Liang, J. O., Fekany, K., Solnickakrezel, L., Korzh, V., Halpern, M. E. and Wright, C. V. E. (1998). Induction of the zebrafish ventral brain and floorplate requires *cyclops/nodal* signalling. *Nature* **395**, 185-189.
- Sasai, Y., Lu, B., Piccolo, S. and De Robertis, E. D. (1996). Endoderm induction by the organizer-secreted factors *chordin* and *noggin* in *Xenopus* animal caps. *EMBOJ.* **15**, 4547-4555.
- Sasaki, H. and Hogan, B. L. (1993). Differential expression of multiple *fork head* related genes during gastrulation and axial pattern formation in the mouse embryo. *Development* **118**, 47-59.
- Schulte-Merker, S., Ho, R. K., Herrmann, B. G. and Nüsslein-Volhard, C. (1992). The protein product of the zebrafish homologue of the mouse T gene is expressed in nuclei of the germ ring and the notochord of the early embryo. *Development* **116**, 1021-1032.
- Shih, J. and Fraser, S. E. (1995). Distribution of tissue progenitors within the shield region of the zebrafish. *Development* **121**, 2755-2765.
- Shimamura, K. and Rubenstein, J. L. R. (1997). Inductive interactions direct early regionalization of the mouse forebrain. *Development* **124**, 2709-2718.
- Stainier, D. Y. R., Lee, R. K. and Fishman, M. C. (1993). Cardiovascular development in the zebrafish: I. Myocardial fate map and heart tube formation. *Development* **119**, 31-40.
- Storey, K. G., Selleck, M. A. and Stern, C. D. (1995). Neural induction and regionalization by different subpopulations of cells in Hensen's node. *Development* **121**, 417-428.
- Strähle, U., Blader, P., Henrique, D. and Ingham, P. W. (1993). *axial*, a zebrafish gene expressed along the developing body axis, shows altered expression in *cyclops* mutant embryos. *Genes Dev.* **7**, 1436-1446.
- Sulik, K., Dehart, D. B., Inagaki, T., Carson, J. L., Vrablic, T., Gesteland, K. and Schoenwolf, G. C. (1994). Morphogenesis of the murine node and notochordal plate. *Dev. Dyn.* **201**, 260-278.
- Thisse, C., Thisse, B., Halpern, M. E. and Postlethwait, J. H. (1994). *goosecoid* expression in neuroectoderm and mesendoderm is disrupted in zebrafish *cyclops* gastrulas. *Dev. Biol.* **164**, 420-429.
- Trevarrow, B., Marks, D. L. and Kimmel, C. B. (1990). Organization of hindbrain segments in the zebrafish embryo. *Neuron* **4**, 669-679.
- Warga, R. M. and Kimmel, C. B. (1990). Cell movements during epiboly and gastrulation in zebrafish. *Development* **108**, 569-580.
- Warga, R. M. and Nüsslein-Volhard, C. (1998). *spadetail*-dependent cell compaction of the dorsal zebrafish blastula. *Dev. Biol.* **203**, 116-121.
- Weigel, D., Jürgens, G., Küttner, F., Seifert, E. and Jäckle, H. (1989). The homeotic gene *fork head* encodes a nuclear protein and is expressed in the terminal regions of the *Drosophila* embryo. *Cell* **57**, 645-658.
- Woo, K. and Fraser, S. E. (1995). Order and coherence in the fate map of the zebrafish nervous system. *Development* **121**, 2595-2609.
- Wood, A. and Thorogood, P. (1984). An analysis of *in vivo* cell migration during teleost fin morphogenesis. *J. Cell Science* **66**, 205-222.
- Wylie, C. C., Snape, A., Heasman, J. and Smith, J. C. (1987). Vegetal pole cells and commitment to form endoderm in *Xenopus laevis*. *Dev. Biol.* **119**, 496-502.